Eur. Phys. J. D **17**, 351–363 (2001)

THE EUROPEAN PHYSICAL JOURNAL D

EDP Sciences

Instanton approach to Josephson tunneling between trapped condensates

Y.-B. Zhang[1,2,a] and H.J.W. Müller-Kirsten[1,b]

[1] Department of Physics, University of Kaiserslautern, 67653 Kaiserslautern, Germany
[2] Department of Physics and Institute of Theoretical Physics, Shanxi University, Taiyuan 030006, P.R. China

Received 29 June 2001 and Received in final form 17 September 2001

Abstract. An instanton method is proposed to investigate the quantum tunneling between two weakly-linked Bose-Einstein condensates confined in double-well potential traps. We point out some intrinsic pathologies in the earlier treatments of other authors and make an effort to go beyond these very simple zero order models. The tunneling amplitude may be calculated in the Thomas-Fermi approximation and beyond it; we find it depends on the number of the trapped atoms, through the chemical potential. Some suggestions are given for the observation of the Josephson oscillation and the MQST.

PACS. 03.75.Fi Phase coherent atomic ensembles; quantum condensation phenomena – 05.30.Jp Boson systems – 32.80.Pj Optical cooling of atoms; trapping

1 Introduction

The first experimental observations of Bose-Einstein condensation (BEC) in dilute gases of trapped alkali atoms [1] have stimulated the studies of condensates in double well traps. With a fascinating possibility of the observation of new kinds of macroscopic quantum phenomena [2], which are related to the superfluid nature of the condensates, numerous authors have addressed this subject area both experimentally and theoretically. Some recent experiments have investigated the relative phase of two overlapping condensates in different hyperfine states [3] and robust interference fringes between two freely expanding condensates have been observed [4] after switching off the double-well potential that confines them, indicating phase coherence both in space and time. In fact the possibility of condensate tunneling between two adjacent atomic traps and detection of Josephson-like current phase effects have been previously suggested [5–7] and intensively studied by two main approaches which are capable of dealing with quantum tunneling in this variant of the Josephson effect. Authors with a quantum optics background tend to favor models in which two boson modes are involved, the so-called two-mode model [8–15]. The other category of theories is based on using the differences of condensate phases and atom numbers between the two sides of the trap as conjugate quantum variables [16]. A detailed comparison between these two approaches is given in reference [17].

The superfluid nature of condensates can be fully tested only through the observation of superflows. Despite the many experimental efforts being focused on the creation of a Josephson junction between two condensate bulks, direct experimental evidences for the atomic oscillation are still far from being realized. Theoretically the Josephson junction problem has been studied in the limit of noninteracting atoms for small-amplitude Josephson oscillations [5,6], including finite-temperature (damping) effects [16]. Dynamic processes of splitting a condensate by raising a potential barrier in the center of a harmonic trap [17,18] and decoherence effects and quantum corrections to the semiclassical mean-field dynamics [8,12,19,20] have also been studied. It has been pointed out [9] that even though the Bose Josephson Junction (BJJ) is a neutral-atom system, it can still display the typical ac and dc Josephson effects occurring in charged cooper-pair superconducting junctions. Moreover, a novel nonlinear effect has been predicted to occur in this BJJ: the self-trapping of a BEC population imbalance arises because of the interatomic nonlinear interaction in the Bose gas [8,9]. This was considered to be a novel "macroscopic quantum self-trapping" (MQST) and was predicted to be observable under certain experimental conditions. Three related parameters, *i.e.* the ground state energy E^0, the interaction energy U, and more importantly, the tunneling amplitude K, are still undetermined for a specific geometry of the potential well and have been taken as constants in references [8,9]. It is the main purpose of this paper to present a rigorous derivation of these quantities and we find that they actually depend on the number of atoms N. This N-dependence refines the conclusions and makes the self-trapping easier to observe.

We develop the instanton method for a sensitive and precise investigation of the tunneling between two

[a] e-mail: ybzhang@physik.uni-kl.de
[b] e-mail: mueller1@physik.uni-kl.de

condensates. The almost trivially looking problem of the tunneling behavior in a double-well potential has attracted much attention from theorists for decades. For a single particle, the solution can be found even in quantum mechanics textbooks [21]. The advantage of a nonperturbative method, as presented here, is that it gives not only a more accurate description of the tunneling phenomena but also a comprehensive physical understanding in the context of quantum field theory. The periodic instanton configurations, which have been shown to be a useful tool in several areas of research such as spin tunneling [22,23], bubble nucleation [24] and string theory [25], enable also the investigation of the finite temperature behavior of these systems. In the case of the Bose-Einstein system, however, we need to evaluate the tunneling frequency for a finite chemical potential even at zero temperature, due to the nonlinear interaction between the confined atoms. Therefore the chemical potential here replaces the position of the excited energy and gives rise to an expected higher tunneling frequency.

Thus, in this paper we will study the atomic tunneling between two condensates in a double-well trap, with special attentions paid to the N-dependent tunneling amplitude. In Section 2 we summarize 3 critical conditions which are related to the MQST effect in the two-mode model. Analytical solutions to the coupled nonlinear BJJ equations are derived in Section 3 and some novel features about the different modes of MQST are discussed in detail. We calculate the three related parameters in the BJJ tunneling system in the Thomas-Fermi Approximation (TFA) and the corrections beyond it in Section 4, in particular, the tunneling amplitude/frequency between the two condensates. We find they actually depend on the number of the trapped atoms through the chemical potential. Our results can be compared to the simple single-particle tunneling result in reference [8] and we find that the latter corresponds to the low-energy or noninteracting case. A detailed discussion about the optimal condition for observation of the MQST and the Josephson tunneling is the subject of Section 5 where some comments are made to the maximum amplitude of the oscillation. Finally our summary and conclusions are given in Section 6.

2 Two-mode model and macroscopic quantum self-trapping

At zero temperature the condensate dynamics can be well described by the Gross-Pitaevskii equation (GPE)

$$\mathrm{i}\hbar\frac{\partial\Phi}{\partial t} = -\frac{\hbar^2}{2m}\nabla^2\Phi + \left[V_{\mathrm{ext}}(\mathbf{r}) + g_0\left|\Phi\right|^2\right]\Phi \qquad (1)$$

where V_{ext} is the external trapping potential and $g_0 = 4\pi\hbar^2 a/m$ is the interatomic coupling constant, with a, m the atomic scattering length and mass, respectively. In this paper we will consider systems interacting with repulsive forces with $a > 0$. To obtain the ground state properties, one can write the macroscopic wave function (or from the viewpoint of phase transitions, the order parameter) of the condensate as $\Phi(\mathbf{r},t) = \phi(\mathbf{r})\mathrm{e}^{-\mathrm{i}\mu t/\hbar}$, where a condensate in the stationary state was assumed. Then the GPE (1) becomes

$$\mu\phi(\mathbf{r}) = \left(\hat{H}_0 + g_0\phi^2(\mathbf{r})\right)\phi(\mathbf{r}),$$
$$\hat{H}_0 = -\frac{\hbar^2\nabla^2}{2m} + V_{\mathrm{ext}}(\mathbf{r}) \qquad (2)$$

with $\hat{H}_0$ the Hamiltonian for the condensates of noninteracting bosons. This equation explains the significance of the chemical potential μ as an energy of the stationary level and can be used further for calculation of the coupling between two condensates, say, the tunneling amplitude (transfer matrix element or Josephson tunneling term) as will be shown below.

Consider a double-well trap produced, for example, by a far-off-resonance laser barrier that cuts a single trapped condensate into two parts. In the two-mode approximation, the condensate dynamics is described by the following BJJ equations [9,10]

$$\mathrm{i}\hbar\frac{\partial\psi_1}{\partial t} = (E_1 + U_1N_1)\,\psi_1 - K\psi_2,$$
$$\mathrm{i}\hbar\frac{\partial\psi_2}{\partial t} = (E_2 + U_2N_2)\,\psi_2 - K\psi_1, \qquad (3)$$

where damping and finite temperature effects are ignored and a two-mode variational ansatz is assumed

$$\Phi(\mathbf{r},t) = \psi_1(t)\Phi_1(\mathbf{r}) + \psi_2(t)\Phi_2(\mathbf{r}). \qquad (4)$$

Here the complex coefficients $\psi_i(t) = \sqrt{N_i(t)}\exp[\mathrm{i}\theta_i(t)]$ are spatially uniform and contain all of the time dependence, while the two states $\Phi_1(\mathbf{r})$ and $\Phi_2(\mathbf{r})$ are localized in the left and right wells, respectively, and contain all of the position dependence. The total number of atoms is conserved in the macroscopic quantum tunneling process, *i.e.*, $N_1+N_2 = |\psi_1|^2+|\psi_2|^2 = N_{\mathrm{T}}$. In the BJJ equation (3), $E_{1,2}$ are the zero-point energies in each well,

$$E_{1,2} = \int \mathrm{d}\mathbf{r}\,\Phi_{1,2}(\mathbf{r})\hat{H}_0\Phi_{1,2}(\mathbf{r}), \qquad (5)$$

U_iN_i are proportional to the atomic self-interaction energies, with

$$U_{1,2} = g_0\int \mathrm{d}\mathbf{r}\,\Phi_{1,2}^4(\mathbf{r}) \qquad (6)$$

and K describes the amplitude of the tunneling between condensates

$$K = -\int \mathrm{d}\mathbf{r}\,\Phi_1(\mathbf{r})\hat{H}_0\Phi_2(\mathbf{r}). \qquad (7)$$

These quantities, which are expressed in terms of appropriate overlap integrals of the wave-functions $\Phi_{1,2}(\mathbf{r})$, have been taken as constants in the previous works and it is one of the main tasks of this paper to obtain them analytically, provided that a specific geometry of the trap is given. We further note that the (real) ground state solutions $\Phi_{1,2}(\mathbf{r})$

for isolated traps with equal population in each well, *i.e.* $N_1 = N_2 = N_T/2$, satisfy the orthonormality condition

$$\int \mathrm{d}\mathbf{r}\, \Phi_i(\mathbf{r})\Phi_j(\mathbf{r}) = \delta_{ij}. \tag{8}$$

For simplicity we restrict our discussions to a symmetric double-well potential, which means that the spatially averaged quantities (5) and (6) are equal for each well. The equations for the relative phase $\phi(t) = \theta_2(t) - \theta_1(t)$ and fractional population imbalance $z = [N_1(t) - N_2(t)]/N_T$ reduce to [9,10]

$$\begin{aligned} \dot{z}(t) &= -\sqrt{1-z(t)^2}\sin\phi(t), \\ \dot{\phi}(t) &= \Lambda z(t) + \frac{z(t)}{\sqrt{1-z(t)^2}}\cos\phi(t), \end{aligned} \tag{9}$$

with the conserved energy

$$\begin{aligned} H &= H[z(t),\phi(t)] = \frac{\Lambda}{2}z(t)^2 - \sqrt{1-z(t)^2}\cos\phi(t) \\ &= H[z(0),\phi(0)] = \frac{\Lambda}{2}z(0)^2 - \sqrt{1-z(0)^2}\cos\phi(0) = H_0. \end{aligned} \tag{10}$$

We have rescaled $2Kt/\hbar$ to a dimensionless time t for time-independent coupling K between two condensates. The parameter Λ, which determines the dynamic regimes of the BEC atomic tunneling, can be expressed as

$$\Lambda = \frac{UN_T}{2K}, \qquad U = (U_1 + U_2)/2. \tag{11}$$

We observe 3 different critical conditions in references [9,10]. One is the MQST condition which is defined by

$$\begin{aligned} &\langle z(t)\rangle \neq 0 \Rightarrow H_0 > 1 \\ &\qquad \Rightarrow \frac{\Lambda}{2}z^2(0) - \sqrt{1-z^2(0)}\cos[\phi(0)] > 1. \end{aligned} \tag{12}$$

In a series of experiments in which $\phi(0)$ and $z(0)$ are kept constant but Λ is varied by changing the geometry or the total number of condensate atoms, we have the critical condition

$$\Lambda > \Lambda_c = \frac{1+\sqrt{1-z(0)^2}\cos\phi(0)}{z(0)^2/2}\,. \tag{13}$$

On the other hand, changing $z(0)$ and keeping $\phi(0)$ and Λ constants we have a critical initial population imbalance

$$z_c = \frac{2}{\Lambda}\sqrt{\Lambda - 1} \tag{14}$$

in both 0-phase mode and π-phase mode case, which describe the tunneling dynamics with the initial or time-averaged value of the phase across the junction being 0 and π, respectively. But for $\phi(0) = 0$, if $z(0) > z_c$, MQST sets in, and for $\phi(0) = \pi$, $z(0) < z_c$ marks the region of MQST. In Figure 1 we show the parameter range for the appearance of MQST and Josephson tunneling for 0-phase mode,

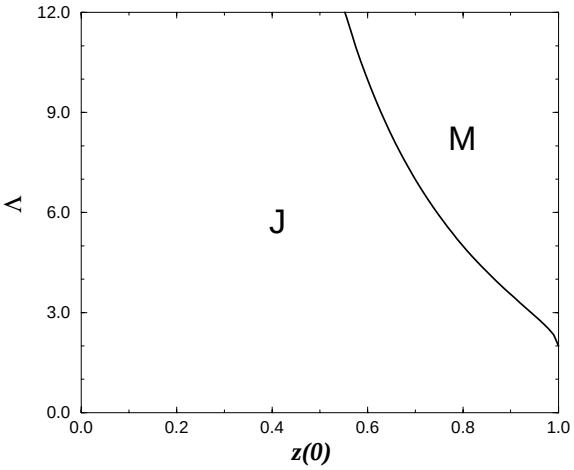

Fig. 1. The parameter range for the appearance of MQST for 0-phase mode: M → MQST, J → Josephson tunneling.

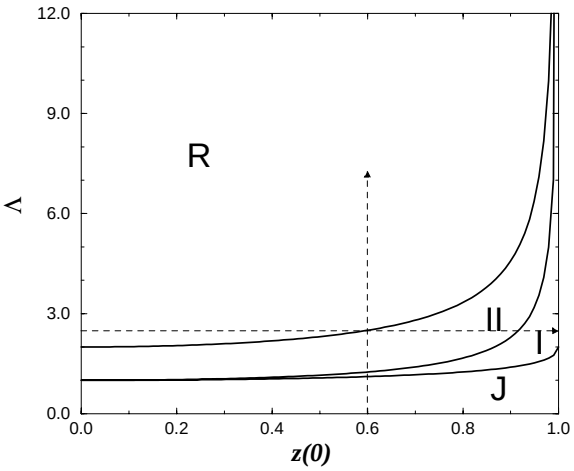

Fig. 2. Different MQST mode for π-phase mode: J → Josephson tunneling, I → MQST Type I, II → MQST Type II, R → MQST unbounded running phase mode. The vertical and horizontal lines correspond to the case of Figures 5 and 7 of reference [10], respectively.

while for the π-phase mode this phase diagram manifests much richer structure as shown in Figure 2. It should be pointed out that the vertical axis Λ can extend to much larger values, but we illustrate in the figure only the area of interest. For $\Lambda > 2$ and $\phi(0) = \pi$, the effective potential $W(z)$ (Eq. (4.13) in Ref. [10]) always has a double-well structure and the system is self trapped for all values of $z(0)$. We conclude that in the case of the π-phase mode the MQST will set in for most of the areas, leaving only a small area for actual Josephson tunneling.

The second condition comes from the stationary z-symmetry-breaking solution [10] the value of z_s is just the boundary of the first- and the second-type of trapped states which differ by the time-average value of the population imbalance $\langle z\rangle$. We enter into some detail of the π phase mode. According to [10], there are two kinds of such

π-phase modes with MQST:

$$\begin{aligned} &\pi\text{-phase modes MQST Type I} \Leftrightarrow \langle z\rangle < z_{\rm s} \neq 0 \\ &\pi\text{-phase modes MQST Type II} \Leftrightarrow \langle z\rangle > z_{\rm s} \neq 0 \end{aligned} \quad (15)$$

with $z_{\rm s}$ being the stationary z-symmetry breaking value of the BJJ equations (3). Once Λ exceeds the value

$$\Lambda_{\rm s} = \frac{1}{\sqrt{1-z^2(0)}}, \quad (16)$$

a changeover occurs at the stationary state and the system goes from Type I of the π-phase trapped state into Type II. In the phase plane portrait of the dynamical variables z and ϕ (Fig. 7 in Ref. [10]) for the fixed value of $z(0) = 0.6$, this critical condition corresponds to the 4 point-like trajectories located at $(\pm\pi, \pm 0.6)$. However, in consideration of the case of a fixed value of Λ, for example, Figures 5c and 5d in reference [10], we find that this definition of the Type I and Type II π-phase modes will lead to a dilemma in the analysis of the phase diagrams and modification to this definition becomes necessary. We return to this point in the following section.

The third condition defines whether the phase $\phi(t)$ is an unbounded running mode or is localized around π. Again from the $z \sim \phi$ phase diagram we know this boundary line can be determined as

$$\phi|_{z=\pm 1} = \frac{\pi}{2}, \qquad \frac{{\rm d}\phi}{{\rm d}z}|_{z=\pm 1} = 0 \Rightarrow \frac{\Lambda}{2} = H_0 \quad (17)$$

which gives the critical values

$$\Lambda_3 = \frac{2}{\sqrt{1-z^2(0)}}, \qquad \text{or} \qquad z_3 = \sqrt{1-\frac{4}{\Lambda^2}}\,. \quad (18)$$

In Figure 2, we managed to give a phase diagram for the π-phase mode, with special attention paid to different MQST modes. Here the area J shows again the Josephson tunneling area, others are 3 MQST areas, with area I the bounded MQST of Type I, area II the Type II, and area R the unbounded running phase mode, respectively. We used the formulae (13, 16, 18) for these three curves, from the bottom up, respectively. We point out that the second and the third conditions apply only to the $\phi(0) = \pi$ case.

3 Exact analytic solutions and different MQST modes

In order to see the oscillations of the fractional population imbalance and the different kinds of (running- and π-phase) MQST modes more transparently, we introduce an effective classical particle whose coordinate is z, moving in a potential $W(z)$ with the initial energy W_0. The effective equation of motion is

$$\dot{z}(t)^2 + W(z) = W_0 \quad (19)$$

where

$$W(z) = z^2\left(1 - \Lambda H_0 + \frac{\Lambda^2}{4}z^2\right), \quad (20)$$

$$W_0 = 1 - H_0^2 = W[z(0)] + \dot{z}(0)^2. \quad (21)$$

We can easily obtain the real time exact solutions in terms of the Jacobian elliptic functions cn and dn. This has been done in references [10,11] but there are some notation errors in the corresponding expressions. We thus rewrite the solutions here and present a detailed discussion, especially on some featured oscillation modes. For the parameters in the area of Josephson tunneling the population imbalance oscillates sinusoidally or nonsinusoidally between a positive initial value C and a negative one $-C$,

$$z(t) = C\,{\rm cn}\left(\frac{C\Lambda}{2k}(t-t_0), k\right) \quad (22)$$

where

$$\begin{aligned} C^2 &= \frac{2}{\Lambda^2}\left((H_0\Lambda - 1) + \frac{\zeta^2}{2}\right), \\ \alpha^2 &= \frac{2}{\Lambda^2}\left(\frac{\zeta^2}{2} - (H_0\Lambda - 1)\right), \\ \zeta^2 &= 2\sqrt{\Lambda^2 + 1 - 2H_0\Lambda} \end{aligned} \quad (23)$$

with $0 < k < 1$ the elliptic modulus,

$$k^2 = \frac{C^2}{\alpha^2 + C^2} = \frac{1}{2}\left(\frac{C\Lambda}{\zeta}\right)^2 = \frac{1}{2}\left(1 + \frac{H_0\Lambda - 1}{\sqrt{\Lambda^2 + 1 - 2H_0\Lambda}}\right). \quad (24)$$

In the case of MQST, however, the elliptic function cn will be replaced by its counterpart dn and the oscillation is about a nonzero average value $\langle z\rangle$

$$z(t) = C\,{\rm dn}\left(\frac{C\Lambda}{2}(t-t_0), 1/k\right). \quad (25)$$

From this we know the value $z(t) = 0$ is inaccessible at any time and the modulus is now $1/k$ with $k > 1$. The integration constant t_0 can be determined from $z(t)|_{t=0} = z(0)$:

$$t_0 = \frac{2k}{C\Lambda}{\rm cn}^{-1}\left(\frac{z(0)}{C}, k\right) = \frac{2}{\Lambda\sqrt{\alpha^2 + C^2}}F\left(\arccos\frac{z(0)}{C}, k\right) \quad (26)$$

where $F(\phi, k) = \int_0^\phi {\rm d}\phi(1 - k^2\sin\phi)^{-1/2}$ is the incomplete elliptic integral of the first kind. Noting the following correspondence

$$\begin{aligned} &0 < k < 1,\ \alpha^2 > 0,\ H_0 < 1, && \text{Josephson oscillation} \\ &k > 1,\ \alpha^2 < 0,\ H_0 > 1, && \text{MQST} \end{aligned} \quad (27)$$

we easily derive the physical condition for the onset of MQST, *i.e.*, $H_0 = 1$ and $\Lambda = \Lambda_{\rm c}$, from the mathematical condition $k = 1$, where the character of the elliptic function solution changes. The Jacobian elliptic functions

$\mathrm{cn}(u,k)$ and $\mathrm{dn}(u,k)$ are periodic in the argument u with period $4\mathcal{K}(k)$ and $2\mathcal{K}(k)$, respectively, where $\mathcal{K}(k)$ is the complete elliptic integral of the first kind. The time period of the oscillation of $z(t)$ is then given by

$$\tau = \frac{2k}{C\Lambda} 4\mathcal{K}(k), \quad \text{for} \quad 0 < k < 1, \tag{28}$$

$$\tau = \frac{2}{C\Lambda} 2\mathcal{K}(1/k), \quad \text{for} \quad k > 1. \tag{29}$$

In the limit of small amplitude, or linear oscillations, $k \to 0$, $K(k) \to \pi/2$, we have

$$\tau = \frac{2\pi}{\sqrt[4]{\Lambda^2 + 1 - 2H_0\Lambda}}\,. \tag{30}$$

For $0,\pi$-phase oscillations, $H_0 \to \mp 1$, the periods in scaled units $2Kt/\hbar$ become

$$\tau = \frac{2\pi}{\sqrt{1 \pm \Lambda}}, \tag{31}$$

respectively, which agree with the unscaled ones (Eqs. (4.7, 4.10) in Ref. [10])

$$\tau_{0,\pi}^{-1} = \sqrt{4K^2 \pm 2UN_{\mathrm{T}}K}/2\pi\hbar. \tag{32}$$

We consider here two special cases, *i.e.*, the $0,\pi$-phase modes. For the 0-phase mode, by inserting $\phi(0) = 0$ into equation (23), we may show that the oscillation amplitude of $z(t)$ is just the initial value $z(0)$,

$$C = z(0). \tag{33}$$

On the other hand, for the π-phase mode, this amplitude will depend on the values of Λ and $z(0)$,

$$\begin{aligned} C^2 &= z^2(0), \qquad \text{when } \Lambda < \Lambda_{\mathrm{s}} \text{ or } z(0) > z_{\mathrm{s}}, \\ C^2 &= z^2(0) + \frac{4}{\Lambda^2}\left[\Lambda\sqrt{1 - z^2(0)} - 1\right], \\ &\qquad \text{when } \Lambda > \Lambda_{\mathrm{s}} \text{ or } z(0) < z_{\mathrm{s}}. \end{aligned} \tag{34}$$

In the case of Josephson tunneling for both 0- and π-phase modes, that is, when the oscillation is in the form of elliptic function cn-type, we always have $C = z(0)$. The reason is that under the condition $\Lambda > \Lambda_{\mathrm{s}}$ or $z(0) < z_{\mathrm{s}}$ for π-phase mode the system is obviously in the region of MQST Type II. Therefore we should use the elliptic function dn for MQST instead. Generally for MQST the average population imbalance may be calculated as (the elliptic function dn oscillates between 1 and k'_{dn})

$$\begin{aligned} \langle z\rangle &= \frac{C}{2}\left(1 + k'_{\mathrm{dn}}\right) = \frac{C}{2}\left(1 + \sqrt{1 - 1/k^2}\right) \\ &= \frac{C}{2}\left(1 + \sqrt{1 - \frac{2\zeta^2}{C^2\Lambda^2}}\right). \end{aligned} \tag{35}$$

For the 0-phase mode, $C = z(0)$ and $\zeta^2 = 2(\Lambda\sqrt{1 - z^2(0)} + 1)$, the average population imbalance is

$$\langle z\rangle = \frac{z(0)}{2}\left(1 + \sqrt{1 - \frac{4\left(\Lambda\sqrt{1 - z^2(0)} + 1\right)}{z(0)^2\Lambda^2}}\right). \tag{36}$$

We take the values of Figure 2 of reference [10] as an example, $\Lambda = 10, z(0) = 0.65, \langle z\rangle = 0.46511$, which is exactly the case. For the π-phase mode, there are two cases.

Case I: $\Lambda < \Lambda_{\mathrm{s}}$ or $z(0) > z_{\mathrm{s}}$ we have $C = z(0)$ and $\zeta^2 = 2\left(1 - \Lambda\sqrt{1 - z^2(0)}\right)$ which give the average population imbalance as

$$\langle z\rangle = \frac{z(0)}{2}\left(1 + \sqrt{1 - \frac{4\left(1 - \Lambda\sqrt{1 - z^2(0)}\right)}{z(0)^2\Lambda^2}}\right). \tag{37}$$

For the parameter in Figure 3d of reference [10], $z(0) = 0.6, \Lambda = 1.2, \langle z\rangle = 0.54944 < 0.6$. This is again exactly the case.

Case II: $\Lambda > \Lambda_{\mathrm{s}}$ or $z(0) < z_{\mathrm{s}}$ we have

$$\begin{aligned} C^2 &= z^2(0) + \frac{4}{\Lambda^2}\left[\Lambda\sqrt{1 - z^2(0)} - 1\right], \\ \zeta^2 &= 2\left(\Lambda\sqrt{1 - z^2(0)} - 1\right), \end{aligned} \tag{38}$$

the average population imbalance is the same as that in Case I, equation (37). For Figure 3f of reference [10], $z(0) = 0.6, \Lambda = 1.3, \langle z\rangle = 0.63715 > 0.6$.

We may compare our phase diagram Figure 2 with those previously known results. First we have a look at the Figure 7 of reference [10], which illustrated the behavior of the system in the $z - \phi$ phase-plane, and concentrating only on the π-phase mode. At a fixed value of $z(0) = 0.6$, increasing the value of Λ will bring the system from area J to area I (Type I bounded MQST with $\langle z\rangle < 0.6$), then area II (Type II bounded MQST with $\langle z\rangle > 0.6$), and finally into the running mode area. This process is described by a vertical line in Figure 2 and it intersects successively the three curves at

$$\Lambda_{\mathrm{c}} = 10/9 = 1.\dot{1}, \qquad \Lambda_{\mathrm{s}} = 1.25, \qquad \Lambda_3 = 2.5, \tag{39}$$

from the bottom up. In Table 1 we list detailed descriptions and graphical features of the oscillations in accordance with Figure 7 of reference [10]. The coincidence here is obvious.

Secondly we go through Figure 5 of reference [10] to see what happens if we keep the value of Λ constant and increase $z(0)$. This is indicated in Figure 2 by a horizontal line. For small values of $z(0)$, the phase is unbounded and the system exhibits running phase MQST. However, above a certain value $z_3 = \sqrt{1 - 4/\Lambda^2}$ (*cf.* Λ_3; there is an error in reference [10] where the condition $z(0) = 2z_{\mathrm{s}} = 2\sqrt{1 - 1/\Lambda^2}$ is unphysical since it is larger than 1), with $\langle z\rangle$ still nonzero, the phase becomes localized around π and remains bounded for all larger values of $z(0)$. Then the puzzle appears here. According to reference [10], in their Figures 5c and 5d, $z(0) = 0.7$ and 0.98 mark the two different types of π-phase MQST since they are on either side of the stationary state value of $z_{\mathrm{s}} = \sqrt{1 - 1/\Lambda^2}$. In this case, along the direction of the horizontal line from left to right, we should enter Type I first ($z(0) = 0.7 < 0.92$),

Table 1. Different oscillation modes for fixed value $z(0) = 0.6$.

$\phi(0) = \pi$	Descriptions	Graphics
$\Lambda = 0$	Rabi oscillation around $\langle z\rangle = 0$	O
$0 < \Lambda < \Lambda_c$	sinusoidal/nonsinusoidal oscillation around $\langle z\rangle = 0$	0
$\Lambda = \Lambda_c = 1.111$	the trajectory shrinks and is pinched at the point $z = 0$ marking the onset of π-phase MQST Type I with $\langle z\rangle < z(0)$	8
$\Lambda_c < \Lambda < \Lambda_s$	upon further increasing the area are divided into 2 parts	° °
$\Lambda = \Lambda_s = 1.25$	the 2 divided areas collapse to 2 point-like trajectories at $z = 0.6$; boundary between MQST Type I and Type II	• •
$\Lambda_s < \Lambda < \Lambda_3$	further increase of Λ induces a reflection of the trajectory about the fixed point and π-phase MQST Type II with $\langle z\rangle > z(0)$	° °
$\Lambda = \Lambda_3 = 2.5$	boundary between bounded-mode (Type II) and running-mode MQST	▽ △
$\Lambda > \Lambda_3$	the trajectory joins the unbounded running-mode MQST	ω m

then Type II ($z(0) = 0.98 > 0.92$). But this is not the case, instead we enter Type II first. The horizontal line cuts the two curves at $z_3 = 0.6$ and $z_s = 0.92$, with the latter corresponding to a point-like trajectory in Figure 5d of reference [10] at $z = 0.92, \phi = \pi$. Another possibility is that although the initial value $z(0) = 0.7 < 0.92$ but the average value $\langle z\rangle > 0.92$. However, from equation (37), we find that in both cases, *i.e.* for $z(0) = 0.7$ and 0.98, we have $\langle z\rangle < 0.92$.

A solution to this dilemma is to define the MQST Types I and II as follows:

$$\begin{aligned} \text{MQST Type I} &\Leftrightarrow \langle z\rangle < z(0) \\ \text{MQST Type II} &\Leftrightarrow \langle z\rangle > z(0) \end{aligned} \tag{40}$$

instead of (15). Under this novel definition we can explain the phase diagrams as follows: for $z(0) = 0.7$ the average population difference $\langle z\rangle > 0.7$ which is obviously Type II, while for $z(0) = 0.98$ we have $\langle z\rangle < 0.98$ which is Type I according to this definition. Therefore, along the direction of the horizontal line from left to right, we enter Type II first ($\langle z\rangle > z(0) = 0.7$), then Type I ($\langle z\rangle < z(0) = 0.98$). At the threshold point, the average value coincides with the initial value, $\langle z\rangle = z(0) = z_s = 0.92$, and the trajectory shrinks to a point. We also notice that the oscillation trajectories for $z(0) = 0.8$ and 0.98 are the same. However, they belong to different regions of MQST. In Table 2 we illustrate the oscillation behavior of a π-phase mode when the value of $z(0)$ is increased while keeping $\Lambda = 2.5$, which can be regarded as an additional remark to Figures 5c and 5d in reference [10]. A further evidence of the correctness of the criterion (40) comes from the fact that from the analytical result for the average population imbalance in the π-phase mode, that is, equation (37), we can derive the second critical condition for Λ,

$$\langle z\rangle = z(0) \Rightarrow \Lambda_s = \frac{1}{\sqrt{1 - z^2(0)}} \tag{41}$$

which agrees with equation (16). And in the case of the 0-phase mode there is no solution for $\langle z\rangle = z(0)$ with $\langle z\rangle$ determined by equation (36), indicating that the self-trapping can only appear as MQST Type I ($\langle z\rangle < z(0)$).

4 Calculation of the tunneling amplitude between two trapped condensates

The macroscopic wave function Φ associated with the ground state of a dilute Bose gas confined in the potential $V_{\rm ext}(r)$ obeys the GPE (1), which can be obtained alternatively using a variational procedure:

$$\mathrm{i}\hbar\frac{\partial}{\partial t}\Phi = \frac{\delta E}{\delta \Phi^*}, \tag{42}$$

where the energy functional E is defined by

$$\begin{aligned} E[\Phi] &= \int \mathrm{d}^3\mathbf{r}\left[\frac{\hbar^2}{2m}\left|\nabla\Phi\right|^2 + V_{\rm ext}(\mathbf{r})\left|\Phi\right|^2 + \frac{g_0}{2}\left|\Phi\right|^4\right] \\ &= E_{\rm kin} + E_{\rm ho} + E_{\rm int}. \end{aligned} \tag{43}$$

The three terms in the integral are the kinetic energy of the condensate $E_{\rm kin}$, the (an)harmonic potential energy $E_{\rm ho}$, and the mean-field interaction energy $E_{\rm int}$, respectively. In the simplest case of an isotropic harmonic trap $V_{\rm ext}(r) = m\omega_0^2 r^2/2$, these energy components, which assume the following simple values in the TFA

$$\frac{E_{\rm kin}}{N} = 0, \qquad \frac{E_{\rm ho}}{N} = \frac{3}{7}\mu_{\rm TF}, \qquad \frac{E_{\rm int}}{N} = \frac{2}{7}\mu_{\rm TF} \tag{44}$$

can be calculated beyond the TFA [2,6,26]

$$\frac{E_{\rm kin}}{N} \simeq \frac{5}{2}C, \quad \frac{E_{\rm ho}}{N} = \frac{3}{7}\mu_{\rm TF} + C, \quad \frac{E_{\rm int}}{N} = \frac{2}{7}\mu_{\rm TF} - C \tag{45}$$

Table 2. The oscillation behavior of a π-phase mode for fixed value $\Lambda = 2.5$.

$z(0)$	The potential $W(z)$	The trajectory ϕ	Descriptions
0	double-well with W_0	pinched	always
	just on the top of the barrier	at $z(0) = 0$	MQST
$0 < z(0) < z_3$	W_0 under the barrier whose	unbounded	running-phase
	height increases with $z(0)$		MQST
$z(0) = z_3 = 0.6$	barrier height increases	$\phi\|_{z=1} = \pi/2$,	boundary between
	continuously with $z(0)$	$\frac{\mathrm{d}\phi}{\mathrm{d}z}\|_{z=1} = 0$	unbounded and localized ϕ
$z_3 < z(0) < z_\mathrm{s}$	barrier height increases	localized	bounded MQST
	continuously with $z(0)$	around π	Type II with $\langle z\rangle > z(0)$
$z(0) = z_\mathrm{s} = 0.92$	barrier attains	shrinks to point-like	boundary between
	its maximum height	trajectory at π	MQST Type I and Type II
$z_\mathrm{s} < z(0) < 1$	barrier height decreases	expands but	bounded MQST
	with increasing $z(0)$	again localized	Type I with $\langle z\rangle < z(0)$
$z(0) = 1$	barrier height decreases to the	agrees	bounded MQST
	same height as $z(0) = 0.6$	with $z(0) = 0.6$	Type I with $\langle z\rangle < z(0)$

where $C = (\hbar^2/mR^2)\ln(R/1.3a_\mathrm{ho})$ is a correction term due to the presence of a boundary layer near the condensate surface. Here N is the number of atoms and the harmonic oscillator length $a_\mathrm{ho} = (\hbar/m\omega_0)^{1/2}$ is introduced for simplicity. Correspondingly the chemical potential in the TFA

$$\mu_\mathrm{TF} = \frac{\hbar\omega_0}{2}\left(15Na/a_\mathrm{ho}\right)^{2/5} \tag{46}$$

which is related to the radius of the condensate R through $\mu_\mathrm{TF} = m\omega_0^2R^2/2$, is modified beyond the TFA as

$$\mu = \mu_\mathrm{TF} + \frac{3}{2}C. \tag{47}$$

First we calculate the two relevant quantities in the Bose Josephson Junction, *i.e.*, the zero-point energy in each well $E_{1,2}$ in equation (5) and the atomic self-interaction energies $U_{1,2}$ in equation (6) both in TFA and beyond it. We note that in the derivation above, the wave function is normalized to N. If one uses instead a wave function normalized to unity, the following correspondence should be realized

$$U_{1,2}N_{1,2} \to 2\frac{E_\mathrm{int}}{N}, \qquad E_{1,2} \to \frac{E_\mathrm{kin}}{N} + \frac{E_\mathrm{ho}}{N}\cdot \tag{48}$$

Setting the initial population difference $z(0) = 0$ as in reference [9], *i.e.*, $N_1 = N_2 = N$, we obtain the ground state energy $E_{1,2}$ and the interaction self energy $U_{1,2}N_{1,2}$ for the isolated traps beyond the TFA

$$E_{1,2} = \frac{3}{7}\mu_\mathrm{TF} + \frac{7}{2}C, \qquad U_{1,2}N_{1,2} = \frac{4}{7}\mu_\mathrm{TF} - 2C, \tag{49}$$

while for TFA the correction terms disappear and these energies take simpler forms

$$E_{1,2} = \frac{3}{7}\mu_\mathrm{TF}, \qquad U_{1,2}N_{1,2} = \frac{4}{7}\mu_\mathrm{TF}. \tag{50}$$

Considering a condensate of $N = 5\,000$ sodium atoms confined in a symmetric spherical trap with frequency $\omega_0 = 100$ Hz, we have the results beyond the TFA, $E_{1,2} = 1.18$ nK, $U_{1,2}N_{1,2} = 1.03$ nK, and in TFA $E_{1,2} = 0.9$ nK, $U_{1,2}N_{1,2} = 1.19$ nK, quite close to the values estimated in reference [9].

In the following we give a rigorous derivation of the amplitude of the atomic tunneling at zero temperature between two nonideal, weakly linked condensates in a double well trap. This induces a coherent, oscillating flux of atoms between wells, that is a signature of the macroscopic superposition of states in which the condensates evolve. To date there have been no reports of experimental observations of Josephson tunneling of a condensate in a double well trap. Josephson tunneling of a condensate in a one dimensional optical lattice was reported in reference [27] and by controlling relative strengths of the tunneling rate between traps and atom-atom interactions within each trap, this technique has been used to produce atom-number-squeezed states in this lattice potential [28]. The analogy of the tunneling mechanism in a two-well potential and an array of wells makes it important to calculate the tunneling amplitude explicitly.

The quantity K in equation (7) corresponds to the tunneling amplitude which can be calculated by different methods, and we demonstrate in this work the use of the nonperturbative instanton approach. The nonlinear interaction between the atoms in the same well will be included, which modifies only the chemical potential μ

both in and beyond the TFA. It is easily shown that this tunneling amplitude is just the quantity $\mathcal{R}$ of [8] (up to a minus sign), if one observes the orthogonality property of the eigenfunctions equation (8), with $\Phi_{1,2}(\mathbf{r})$ the local modes in each well. We study the amplitude for tunneling between the two condensates confined in the wells of an external double-well potential in the 3-dimensional

$$V_{\rm ext}(\mathbf{r}) = \frac{m\omega_0^2}{8x_0^2}(x^2 - x_0^2)^2 + \frac{1}{2}m\omega_0^2 y^2 + \frac{1}{2}m\omega_0^2 z^2 \quad (51)$$

where we have assumed as in reference [8] that the inter-well coupling occurs only along x and the wave function components in the other two dimensions are orthogonal and contribute a factor of unity. The two minima are located at $\pm x_0$ on the x-axis and the parabolic approximation to the potential in the vicinity of each minimum is

$$\tilde{V}^{(2)}(\mathbf{r} - \mathbf{r}_{1,2}) = \frac{1}{2}m\omega_0^2\left[(x \pm x_0)^2 + y^2 + z^2\right]. \quad (52)$$

The barrier height between the two wells

$$V_0 = \frac{1}{8}m\omega_0^2 x_0^2 \quad (53)$$

is assumed to be high enough so that the overlap between the wave functions relative to the two traps occurs only in the classically forbidden region where interaction can be ignored and one can safely use the WKB wave function approximately [6]

$$\Phi_{1,2}(\mathbf{r}) \sim \frac{B}{\left\{2m\left[V_{\rm ext}(r) - \mu\right]\right\}^{1/4}} \times \exp\left(-\sqrt{\frac{2m}{\hbar^2}}\int_R^r \left[V_{\rm ext}(r) - \mu\right]^{1/2} {\rm d}r'\right) \quad (54)$$

with B a properly selected coefficient. The direct integration of K in equation (7) using the above WKB wave functions is quite a difficult task, as already noticed in references [6,16]. In the simplest case the local mode of each well was assigned in reference [8] the harmonic oscillator single particle ground state wave function

$$\Phi_{1,2}(\mathbf{r}) = \left(\frac{m\omega_0}{\hbar\pi}\right)^{1/4}\exp\left(-\frac{m\omega_0}{2\hbar}r^2\right) \quad (55)$$

and the tunneling frequency was obtained through simple integration of these Gaussian wave functions

$$\Omega = \frac{2}{\hbar}\mathcal{R} = \frac{2}{\hbar}\int {\rm d}\mathbf{r}\,\Phi_1^*(\mathbf{r})\left[V_{\rm ext}(\mathbf{r}) - \tilde{V}^{(2)}(\mathbf{r} - \mathbf{r}_{1,2})\right]\Phi_2(\mathbf{r}) = \frac{x_0^2}{a_{\rm ho}^2}\omega_0 {\rm e}^{-x_0^2/a_{\rm ho}^2}. \quad (56)$$

This result, however, is independent of the characteristic parameters of the trapped atoms, such as the number of the atoms, the chemical potential and the interatomic coupling constant, etc. This inadequacy is expected to be cured by means of the periodic instanton method presented in the following.

Alternatively in some references the authors [29] used the external double-well potential in the form

$$V_{\rm ext}(\mathbf{r}) = V_{\rm H}(\mathbf{r}) + V_{\rm B}(\mathbf{r}) \quad (57)$$

which is created by superimposing a harmonic trap

$$V_{\rm H}(\rho, z) = m\omega_z^2\left(\lambda^2\rho^2 + z^2\right)/2 \quad (58)$$

and a Gaussian barrier along the z-axis

$$V_{\rm B}(z) = U_0\exp\left(-\frac{z^2}{2\sigma^2}\right). \quad (59)$$

In their calculations, they considered a range of values for the trap frequencies ω_z and ω_ρ, the barrier height U_0 and width σ, and the condensate population $N_{\rm c}$. In the spherical or 1-dimensional case, one can also consider the time-dependent behavior by means of the variational ansatz [18]. Our observation is that in the vicinity of the tunneling region the above potential in the 1-dimensional case

$$V_{\rm ext}(x) = \frac{1}{2}m\omega_0^2 x^2 + U_0\exp\left(-\frac{x^2}{2\sigma^2}\right) \quad (60)$$

can be well approximated by the double-well (61) considered in this paper for a variety of the geometric parameters of the trap.

Now we turn to the field theory description of the GPE, *i.e.* the periodic instanton method which can not only give the correct exponential contribution of the Euclidean action but also the prefactor. The equal population case with $N_1 = N_2 = N$ is assumed in the following calculations, due to the negligible effect of the slow time evolution of the number of particles $N_i(t)$ [30]. To this end we consider a scalar field problem in a 1-dimensional time plus 1-dimensional space

$$V_{\rm ext}(x) = \frac{m\omega_0^2}{8x_0^2}\left(x^2 - x_0^2\right)^2. \quad (61)$$

After a Wick's rotation $t = -{\rm i}\tau$ the Euclidean-Lagrangian equation of motion for a finite chemical potential takes the form

$$\frac{1}{2}m\left(\frac{{\rm d}x}{{\rm d}\tau}\right)^2 - V_{\rm ext}(x) = -\mu. \quad (62)$$

The reason why we can handle a nonlinear problem by means of a linear equation of motion is that we discuss the tunneling behavior in the barrier region where the nonlinear interaction is negligibly small. However, there are obvious differences between the BEC tunneling system and the usual one-body problem, *i.e.* the nonlinear interaction contributes a finite chemical potential, which is just the integration constant on the right hand side of equation (62). The classical turning points on both sides of the barrier can be determined by the relation $V(x_{1,2}) = \mu$ as suggested in reference [6]. For a noninteracting system the chemical potential approaches the ground state energy corresponding to the vacuum instanton case in [31,32].

Solving this Euclidean time classical equation in the usual way [32] one obtains the periodic instanton solution in terms of the Jacobian elliptic function

$$x_{\rm c} = 2x_0\bar{k}b(\bar{k})/\omega_0 \,{\rm sn}\left(b(\bar{k})\tau, \bar{k}\right) \tag{63}$$

where sn is a Jacobian elliptic function with modulus $\bar{k}$, and the parameters are defined as

$$b(\bar{k}) = \frac{\omega_0}{2}\sqrt{\frac{2}{1+\bar{k}^2}}, \qquad \bar{k}^2 = \frac{1-u}{1+u}, \qquad u = \sqrt{\frac{\mu}{V_0}} \tag{64}$$

with the imaginary time period $T = 2\mathcal{K}(\bar{k})/b(\bar{k})$. The action for the half period can be calculated along the above instanton trajectory (63)

$$S_{\rm c} = \int_{-T/2}^{T/2} {\rm d}\tau \left(\frac{1}{2}m({\rm d}x_{\rm c}/{\rm d}\tau)^2 + V_{\rm ext}(x_{\rm c})\right) = W + \mu T/2 \tag{65}$$

where

$$W = \frac{2}{3}\frac{8V_0}{\omega_0}(1+u)^{1/2}\left(\mathcal{E}(\bar{k}) - u\mathcal{K}(\bar{k})\right). \tag{66}$$

Here $\mathcal{E}(\bar{k})$ denotes the complete elliptic integral of the second kind with modulus $\bar{k}$. The frequency of tunneling between the two condensates is then given by the energy level splitting of the two lowest states, *i.e.* $\Omega = \Delta E/\hbar = 2K/\hbar = 2\mathcal{R}/\hbar$ and can be calculated by means of the path integral method as [32]

$$\Omega = \frac{1}{\hbar}A{\rm e}^{-W/\hbar} = \frac{\sqrt{1+u}}{2K(\bar{k}')}\omega_0 \exp\left[-\frac{W}{\hbar}\right]. \tag{67}$$

We emphasize here that an explicit prefactor A is included in this formula, which has been proven to be valid for the entire region when the chemical potential is below the barrier height. A remarkable feature of this periodic instanton result for the tunneling frequency is that it depends on the chemical potential μ, or equivalently the number of the trapped atoms N through equations (46) or (47). This result will affect the conclusion about the observation of the MQST, as will be shown in next section. When the chemical potential approaches the top of the barrier, *i.e.*

$$V_0 = \mu \tag{68}$$

the periodic instanton solution (63) becomes the trivial configuration $x_{\rm c} = 0$ with a name "sphaleron" which means "ready to fall" [33], where a type of quantum-classical transition may occur [22]. From the equations (46, 53), in the TFA this means

$$x_0 = 2R = 2a_{\rm ho}\left(\frac{15N_{\rm T}a}{2a_{\rm ho}}\right)^{1/5} \tag{69}$$

where $N_{\rm T} = N_1 + N_2$ is the total number of atoms in both wells together. Therefore for a specific type of trapped atoms and a given double-well potential with separation x_0 (the number of atoms $N_{\rm T}$) there exists a critical number of atoms $N_{\rm c1}$ (critical separation $x_{\rm c1}$) determined by the above equation, below (above) which the tunneling process will give the main contribution to the tunneling amplitude. However, above this critical number of atoms or below this critical separation value another process, *i.e.* the over-barrier activation will dominate (which is definitely not "thermal activation" as in spin tunneling since the temperature is zero) (*cf.* Fig. 3). Between these two processes there exists a crossover. A more explicit condition for this critical number of atoms (separation between the two minima) can be derived beyond the TFA from equations (47, 53), *i.e.*

$$x_0 = 2R\sqrt{1 + \frac{3}{5}\left(\frac{15N_{\rm T}a}{2a_{\rm ho}}\right)^{-4/5}\ln\left(\frac{15N_{\rm T}a}{2a_{\rm ho}1.3^5}\right)}. \tag{70}$$

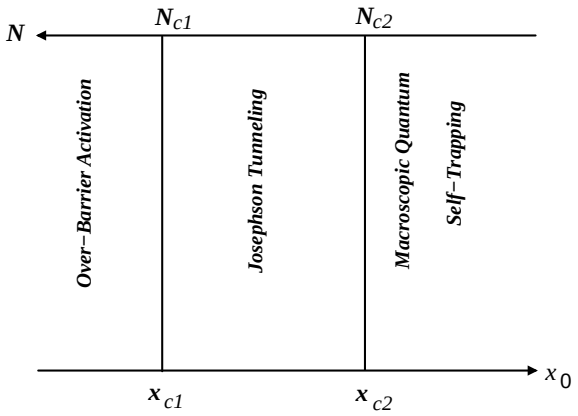

Fig. 3. 3 different processes through which the condensates can interchange atoms with the corresponding critical parameters of the boundaries.

As an example, we consider two weakly-linked condensates of $N_{\rm T} = 10^4$ sodium atoms, confined in two symmetric spherical traps with frequency $\omega_0 = 100$ Hz as in reference [9]. The critical value for $x_{\rm c1}$ is $x_{\rm c1} = 24.58$ μm or more accurately $x_{\rm c1} = 25.29$ μm. We note that here the height of the potential barrier is $V_0 = 2.21$ nK and the ground state is located at $\hbar\omega_0/2 = 0.38$ nK so that there are several energy levels beneath the barrier height. This means the interaction between the atoms contributes to the chemical potential, which effectively raises the classical turning points to a remarkably high level. Although the atoms remain in the ground state, the interaction energy is so strong that the vacuum instanton method can no longer be applied. We have to resort to the periodic instanton method, as will be shown below.

We now consider the "low-energy" or "non-interacting" limit, $\mu \to 0$. As in the case of a uniform Bose gas, the number of atoms in the ground state can be macroscopic, *i.e.*, of the order of the total number in one potential well, when the chemical potential becomes equal to the energy of the lowest state, which, in our 1-dimensional case here, is $\mu \to \mu_{\rm c} = \hbar\omega_0/2$. The lower

boundary for the chemical potential in fact implies that

$$\mu_{\rm c} = \frac{1}{2}\hbar\omega_0 = \frac{1}{2}m_0\omega_0^2 R_{\rm c}^2 \to R_{\rm c} = \sqrt{\frac{\hbar}{m_0\omega_0}} = a_{\rm ho}, \quad (71)$$

i.e. the radius of the condensate should never be less than the harmonic oscillator length $a_{\rm ho}$. We thus have a result similar to that in the vacuum instanton case [32] and the "low energy" limit here is only meaningful in this sense. Expanding equation (67) far below the barrier height, *i.e.*, around the modulus $k \to 1$, or equivalently evaluating the tunneling amplitude in the vacuum instanton method [32], we obtain for the tunneling frequency

$$\Omega = 2\sqrt{\frac{6S_{\rm c}}{\pi\hbar}}\omega_0 \exp\left(-S_{\rm c}/\hbar\right) \quad (72)$$

with the Euclidean action

$$\frac{S_{\rm c}}{\hbar} = \frac{2}{3}\frac{8V_0}{\hbar\omega_0} = \frac{2}{3}\frac{x_0^2}{a_{\rm ho}^2}\,. \quad (73)$$

This result can be compared with that of reference [8], equation (56), which, however, gives not only a smaller exponential contribution

$$\frac{S_{\rm c}}{\hbar} = \frac{8V_0}{\hbar\omega_0} = \frac{x_0^2}{a_{\rm ho}^2}, \quad (74)$$

(there is a 2/3 factor) but also an inaccurate prefactor

$$A = \omega_0 S_{\rm c}/\hbar. \quad (75)$$

The source of this inaccuracy is the adoption of the too simple harmonic oscillator wave function of a single particle, which obviously oversimplifies the Bose-Einstein condensation tunneling problem. At least one should use the WKB wave function (54) in the tunneling region, and it can be shown that this corresponds to the vacuum instanton result we present here. For the agreement between WKB and vacuum instanton methods we refer to reference [34].

We clarify here some features about the two-mode approximation. It is only when there are many energy levels in each well and the barrier height is very large that the tunneling behavior can be well defined. As already pointed out in reference [8], the potential should be such that the two lowest states are closely spaced and well separated from higher levels of the potential, and that many-particle interactions do not significantly change this situation. This assumption permits a two-mode approximation to the many-body description of the system and requires that $x_0 \gg a_{\rm ho}$. In the example considered in reference [8] the harmonic length is estimated to be $a_{\rm ho} = 1.66$ μm for sodium atoms in a double-well trap with $\omega_0 = 1$ kHz. The two-mode approximation requires that there are at least two levels beneath the barrier, *i.e.*

$$V_0 = \frac{1}{8}m\omega_0^2 x_0^2 \gtrsim \frac{3}{2}\hbar\omega_0, \quad (76)$$

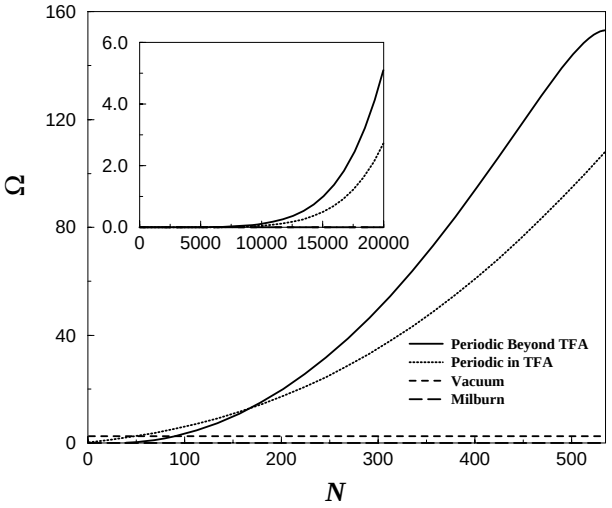

Fig. 4. N-dependence of the tunneling frequency Ω for $\omega = 1$ kHz, $x_0 = 5.76$ μm: solid line is the result of periodic instanton method beyond the TFA, while dashed line that in TFA. The two horizontal lines are the results on noninteracting limit, one corresponds to that of reference [8], another is from the vacuum instanton method. Inset: $\omega = 100$ Hz, $x_0 = 30$ μm. In both cases the constant results are negligibly small comparing to the N-dependent frequencies.

which means the minimum separation x_0 should be larger than 5.76 μm. For this separation equation (56) gives the tunneling frequency $\Omega \sim 0.0737$ Hz, whereas the vacuum instanton result from (72) is $\Omega \sim 2.62$ Hz; however, it is expected to reach 37% of ω_0 in reference [8], that is 370 Hz (from Eq. (56) we know this frequency can be achieved only at a quite small separation $x_0 \sim 1.6$ μm). This is obviously in contradiction. To remedy this, we notice that the periodic instanton result equation (67) can reach a maximum frequency $\Omega \sim 150$ Hz, which is a much higher one but for a quite small number of trapped atoms $N_{\rm c1} \simeq 535$ (Fig. 4). This can be easily understood as follows. The chemical potential for 5×10^5 atoms in the realistic experiment of the MIT group in reference [1], $\mu = 158.35$ nK, lies much higher than the barrier height $V_0 = 11.46$ nK if the two condensates are separated as close as 5.76 μm, leading to an unphysical parameter in equation (64) $u = \sqrt{\mu/V_0}$ which is larger than 1. In this case the periodic instanton method cannot apply and the over barrier activation process will dominate over the Josephson tunneling. In the language of Josephson junction the two condensates seem to be connected directly with each other and no barrier exists between them. From another viewpoint, for the separation smaller than 5.76 μm we cannot put 5×10^5 atoms in the double-well, *i.e.* the barrier seems no longer to exist for so many atoms and one cannot distinguish to which potential well the atoms belong and the oscillation is meaningless. The upper boundary for the trapped number of atoms can be estimated just to be $N_{\rm c1} \simeq 535$ from equation (70).

In Figure 4 we show the N-dependence of the tunneling frequency Ω both for a chemical potential in TFA (46)

and beyond it (47). The periodic instanton results obviously lead to a rapidly growing behavior for the tunneling frequency when the chemical potential, *i.e.* the number of atoms is increased. The results of reference [8] equation (56) and that from the vacuum instanton method equation (72) are also shown as horizontal lines.

5 Observation of macroscopic quantum self trapping

We are now in a position to discuss the optimal conditions for observation of the Josephson oscillation and the MQST effects. According to reference [9], for a fixed value of the initial population imbalance $z(0)$ and phase difference $\phi(0)$, if the parameter Λ exceeds a critical value $\Lambda_{\rm c}$ in equation (13), the population becomes macroscopically self-trapped with a nonzero average population difference $\langle z\rangle$. There are different ways in which this state can be achieved, and all of them correspond to the so-called MQST condition equation (12). Similar results were obtained in reference [8] for the case that all atoms are initially localized in one well and it is concluded that the self-trapping will occur when the total number of the trapped atoms $N_{\rm T}$ exceeds a critical value $N_{\rm c2}$ determined by

$$N_{\rm c2} = \frac{2\hbar\Omega}{g_0} V_{\rm eff} = \frac{4K}{U_{1,2}} \tag{77}$$

where $V_{\rm eff}^{-1} = \int {\rm d}\mathbf{r}\, \Phi_{1,2}^4(\mathbf{r})$ is the effective mode volume of each well. For this special case $z(0) = 1$, the critical value $\Lambda_{\rm c}$ is shown to be $\Lambda_{\rm c} = 2$ for any initial phase difference $\phi(0)$ and equation (77) is obviously identical with the MQST condition $UN_{\rm T} > 4K$ from equation (12).

The parameters $UN_{\rm T}$ and K, however, are considered as N-independent constants in references [8,9]. Considering the fact that they depend actually on the number of the trapped atoms N as in our calculation above, we can refine the conclusions of references [8,9]. To access the region of self-trapping, that is, $\Lambda = UN_{\rm T}/2K > \Lambda_{\rm c}$, it is better to lower the value of K by making a higher barrier height $V_0 = m\omega_0^2 x_0^2/8$ through increasing the separation x_0 or the oscillation frequency ω_0, than to increase the number of atoms as suggested in reference [9]. In fact, the quantity $UN_{\rm T}$ here is proportional to $\mu_{\rm TF} \sim N^{2/5}$ as shown in equations (50, 46), which means that increasing the number of atoms will not increase the interaction energy significantly, and at the same time the tunneling amplitude will be increased more drastically (Fig. 4). Thus, contrary to the observations in references [8,9], we find that the MQST will occur when the number of atoms is smaller (instead of larger) than a critical value $N_{\rm c2}$, *i.e.* we should decrease the number of atoms instead of increasing it (Fig. 3). Inserting the values of the interaction energy equations (50) or (49), the chemical potential equations (46) or (47) and the tunneling amplitude (67) into equation (12) we may obtain this critical number of atoms for a given potential geometry in TFA

$$8\mu_{\rm TF} = 7\Lambda_{\rm c}\hbar\Omega_{\rm TF}, \tag{78}$$

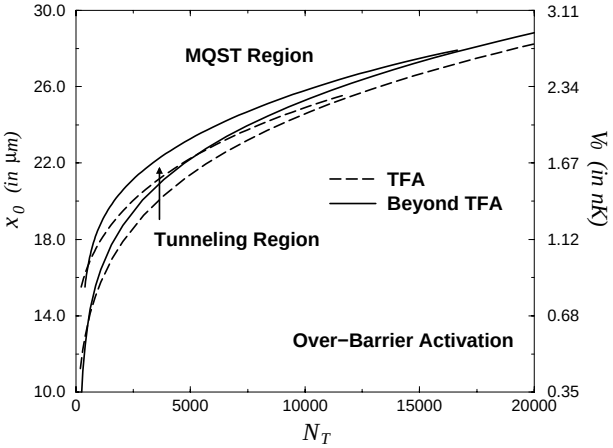

Fig. 5. Critical line for MQST effect. Solid line: results beyond TFA where the parameters take the values $UN_{\rm T} = 8/7\mu_{\rm TF} - 4C$ and $\mu = \mu_{\rm TF} + 3C/2$. Dashed line: TFA results where $UN_{\rm T} = 8/7\mu_{\rm TF}$ and $\mu = \mu_{\rm TF}$ are used in the numerical simulation.

or beyond it

$$8\mu_{\rm TF} - 28C = 7\Lambda_{\rm c}\hbar\Omega_b \tag{79}$$

where $\Omega_{\rm TF}$ and Ω_b are the tunneling frequencies in equation (67) with the chemical potential μ taking the values in TFA and beyond it, respectively.

The parameters which can be adjusted are the number of atoms $N_{\rm T}$, the oscillation frequency ω_0, and the separation distance between the two condensates x_0. Figure 3 shows the three different regions for different numbers of atoms and distances between the potential wells. When x_0 ($N_{\rm T}$) is smaller (larger) than the critical value $x_{2\rm c}$ ($N_{\rm c2}$), the atoms will oscillate between these two potential wells. Once we increase the separation above (or decrease the number of atoms below) this critical value, the MQST will occur, *i.e.*, most of the atoms will tend to remain in their appropriate wells, leading to only a small oscillation around a fixed population difference.

We take the initial condition for the population difference to be $z(0) = 0.4$ and the zero-phase case $\phi(0) = 0$ as an example. Other cases with, for example, a non-zero phase difference give rise to only a different critical parameter $\Lambda_{\rm c}$. For sodium atoms confined in the double-well potential with $\omega_0 = 100$ Hz, we show numerically in Figure 5 the critical line between the three different regions in TFA and beyond it. The upper region marks the self-trapping region, the lower the over-barrier activation. Quantum tunneling occurs only for a small range of the parameter. In the experiment [4], the barrier was generated by an off-resonance (blue detuned) laser beam. To make our results more applicable to experiment we denote on the right vertical axis the corresponding barrier height in units of nK. We also find that the tunneling will be suppressed when the separation or the number of atoms satisfies $x_0 > 28$ μm or $N_{\rm T} > 12\,500$ (in TFA $x_0 > 26$ μm or $N_{\rm T} > 12\,000$). The crossover will occur directly between the self-trapping and the over-barrier regions, quite similar to the first-order transition in spin tunneling [22].

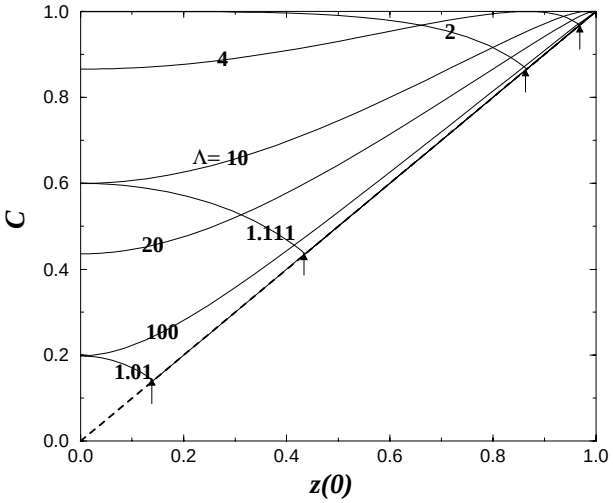

Fig. 6. The oscillation amplitude for 0- and π-phase modes. The slope line is the result of 0-phase mode, whereas others are results for different values of Λ, as indicated in the figure. The arrows indicate the critical value $z_{\rm s}$, which increases with Λ and finally approaches 1 for very large Λ.

The self trapping region is very easy to access considering the easier decrease of the tunneling amplitude.

Secondly, from the solution for $z(t)$ in equations (22, 25) we can define maximum amplitudes of oscillation. For equal populations initially, *i.e.* $z(0) = 0$, we have $H_0 = -\cos\phi(0)$, and the amplitude

$$C = \frac{1}{\Lambda}\Big[2\Big(\sqrt{\Lambda^2 + 1 + 2\Lambda\cos\phi(0)} - \Lambda\cos\phi(0) - 1\Big)\Big]^{1/2}. \tag{80}$$

For $\Lambda > 2$, there is only 1 maximum, *i.e.*, $\phi(0) = \pi$. For $\Lambda < 2$, however, $\phi(0) = \pi$ is a minimum, while two maxima correspond to $\cos\phi(0) = -\Lambda/2$. Consequently from equation (80) we have for $\Lambda > 2$

$$z_{\max} = 2\sqrt{\Lambda - 1}/\Lambda \tag{81}$$

and for $\Lambda < 2$

$$z_{\max} = 1. \tag{82}$$

We claim here that the result for the maximum amplitude equation (26) of reference [29] is not relevant, in which the author erroneously took $\phi(0) = \pi/2$ as a maximum. If instead the initial population difference is nonzero, in reference [29] the author obtained the same result for the maximum amplitude as equation (81) by setting $\phi(0) = 0$ in equation (13). However, we show here this is not true for $\phi(0) = \pi$ because for the π-phase mode it is when $z(0) > 2\sqrt{\Lambda - 1}/\Lambda$ that the Josephson oscillation will occur [10]. In this case equation (81) gives the minimum amplitude instead of the maximum one. As already shown in Section 3, the oscillation amplitude in the 0-phase mode is just the initial value of population imbalance $z(0)$, while in the more interesting π-phase mode, we plot the amplitude equation (34) as a function of $z(0)$ in Figure 6 for different values of Λ. It is clear that the amplitudes in the π-phase mode are always larger than those in the 0-phase mode. The straight slope line is the result of the 0-phase mode. For small values of Λ, the amplitudes join the slope line when $z(0) > z_{\rm s} = \sqrt{1 - 1/\Lambda^2}$, with this critical value $z_{\rm s}$ increasing with Λ, and finally approaching 1 for very large Λ. At a special value of $\Lambda = 2$, it is seen that the oscillation amplitude can reach 1 even for a zero initial population imbalance. For very large Λ the amplitudes in these two cases agree tangentially with each other. However, from Figure 2, the condensates will be self trapped for any initial population imbalance if $\Lambda > 2$, making the Josephson tunneling unobservable.

6 Conclusions

We have shown that the periodic instanton method can be used to investigate the tunneling problem in BEC systems at zero temperature. In particular, some deficiencies of the earlier treatments are removed. First of all, the tunneling amplitude and the nonlinear interaction energy between the atoms which have been taken as constants in references [8,9], are calculated analytically in the Thomas-Fermi approximation and beyond it. The interesting features of the MQST effect are discussed is more detail and we observe the N-dependence of the tunneling amplitude K and the self interaction energy $UN_{\rm T}$. Secondly, the N-dependence of the tunneling frequency Ω manifests a rapidly growing behavior when the chemical potential, *i.e.*, the number of atoms in the trapped condensate is increased. In this sense, the result of reference [8] may be considered as that of a non-interacting approximation. Finally, for the observations of Josephson oscillation and the self trapping effect, we suggest that one should use a small number of trapped atoms and change the barrier height through altering the separation x_0 or the oscillation frequency ω_0 as is evident from the calculation of this paper. Furthermore the π-phase mode, that is, when the relative phase of the wave functions between the two condensates are opposite to each other, favors the observation of MQST, since a somewhat large Λ will bring the system out of the region of Josephson tunneling. To observe the Josephson oscillation it is better one adjusts instead the system into the 0-phase mode.

Recently direct observation of an oscillating atomic current has been reported in a one-dimensional array of Josephson junctions realized with ^{87}Rb atomic condensate [35]. The authors verified that the BEC's dynamics on a lattice is governed by a discrete, nonlinear Schrödinger equation [36] which is common to a large class of nonlinear systems. They used a simple variational estimate, assuming a Gaussian profile for the condensate in each trap, giving the value of tunneling amplitude K, and a chemical potential $\mu \sim 0.06V_0$ that is much lower than the potential barrier V_0. This confirms our prediction that one should use a small number of trapped atoms for the observations of Josephson oscillation. They also observed that the wave functions, as well as K, depend on the barrier height, however, leaving the analytical result unsolved. The instanton

result can be extended to the investigation of the Bose-gas in such a periodic optical lattice [36], the two-component spinor condensates, or even the metastability in the case of attractive interaction. Work along this direction is in progress.

It is a great pleasure to thank J.E. Williams, F. Dalfovo, A. Smerzi, X.-B. Wang, W.-D. Li and J.-Q. Liang for useful discussions. Y.Z. acknowledges support by an Alexander von Humboldt Foundation Fellowship. This research was supported in part by NSFC of China under grant No. 10075032.

References

1. M.H. Anderson, J.R. Ensher, M.R. Matthews, C.E. Wieman, E.A. Cornell, Science **269**, 198 (1995); K.B. Davis, M.-O. Mewes, M.R. Andrews, N.J. van Druten, D.S. Durfee, D.M. Kurn, W. Ketterle, Phys. Rev. Lett. **75**, 3969 (1995); C.C. Bradley, C.A. Sackett, J.J. Tollett, R.G. Hulet, *ibid.* **75**, 1687 (1995).
2. A.S. Parkins, D.F. Walls, Phys. Rep. **303**, 1 (1998); F. Dalfovo, S. Giorgini, L. Pitaevskii, S. Stringari, Rev. Mod. Phys **71**, 463 (1999); A.J. Leggett, Rev. Mod. Phys **73**, 307 (2001).
3. D.S. Hall, M.R. Matthews, C.E. Wieman, E.A. Cornell, Phys. Rev. Lett. **81**, 1543 (1998); M.R. Matthews, B.P. Anderson, P.C. Haljan, D.S. Hall, M.J. Holland, J.E. Williams, C.E. Wieman, E.A. Cornell, *ibid.* **83**, 3358 (1999).
4. M.R. Andrews, C.G. Townsend, H.-J. Miesner, D.S. Durfee, D.M. Kurn, W. Ketterle, Science **275**, 637 (1997).
5. J. Javanainen, Phys. Rev. Lett. **57**, 3164 (1986); S. Grossmann, M. Holthaus, Z. Naturforsch. A **50**, 323 (1995).
6. F. Dalfovo, L. Pitaevskii, S. Stringari, Phys. Rev. A **54**, 4213 (1996).
7. W. Reinhard, C.W. Clark, J. Phys. B: At. Mol. Opt. Phys. **30**, L785 (1997).
8. G.J. Milburn, J. Corney, E.M. Wright, D.F. Walls, Phys. Rev. A **55**, 4318 (1997).
9. A. Smerzi, S. Fantoni, S. Giovanazzi, S.R. Shenoy, Phys. Rev. Lett. **79**, 4950 (1997).
10. S. Raghavan, A. Smerzi, S. Fantoni, S.R. Shenoy, Phys. Rev. A **59**, 620 (1999).
11. S. Raghavan, A. Smerzi, S. Fantoni, S.R. Shenoy, Int. J. Mod. Phys. B **13**, 633 (1999).
12. I. Marino, S. Raghavan, S. Fantoni, S.R. Shenoy, A. Smerzi, Phys. Rev. A **60**, 487 (1999); S. Raghavan, A. Smerzi, V.M. Kenkre, *ibid.* **60**, R1787 (1999); A. Smerzi, S. Raghavan, *ibid.* **61**, 063601 (2000); S. Giovanazzi, A. Smerzi, S. Fantoni, Phys. Rev. Lett. **84**, 4521 (2000).
13. M.W. Jack, M.J. Collett, D.F. Walls, Phys. Rev. A **54**, R4625 (1996).
14. J. Javanainen, M. Wilkens, Phys. Rev. Lett. **78**, 4675 (1997); A.J. Leggett, F. Sols, *ibid.* **81**, 1344 (1998); J. Javanainen, M. Wilkens, *ibid.* **81**, 1345 (1998).
15. J. Ruostekoski, D.F. Walls, Phys. Rev. A **58**, R50 (1998); K. Molmer, *ibid.* **58**, 566 (1998); E.A. Ostrovskaya, Y. Kivshar, M. Lisak, B. Hall, F. Cattani, D. Anderson, *ibid.* **61**, 031601 (2000).
16. I. Zapata, F. Sols, A.J. Leggett, Phys. Rev. A **57**, R28 (1998); A.J. Leggett, F. Sols, Found. Phys. **21**, 353 (1991); F. Sols, Physica B **194-196**, 1389 (1994); S. Kohler, F. Sols, Phys. Rev. A **63**, 053605 (2001).
17. J. Javanainen, M.Yu. Ivanov, Phys. Rev. A **60**, 2351 (1999).
18. C. Menotti, J.R. Anglin, J.I. Cirac, P. Zoller, Phys. Rev. A **63**, 023601 (2001); R.W. Spekkens, J.E. Sipe, *ibid.* **59**, 3868 (1999).
19. A. Imamoglu, M. Lewenstein, L. You, Phys. Rev. Lett. **78**, 2511 (1997); Y. Castin, J. Dalibard, Phys. Rev. A **55**, 4330 (1997); R. Graham, T. Wong, M.J. Collett, S.M. Tan, D.F. Walls, *ibid.* **57**, 493 (1998); J.I. Cirac, M. Lewenstein, K. Molmer, P. Zoller, *ibid.* **57**, 1208 (1998); M.J. Steel, M.J. Collett, *ibid.* **57**, 2920 (1998); P. Villain, M. Lewenstein, *ibid.* **59**, 2250 (1999); F. Meier, W. Zwerger, *ibid.* **64**, 033610 (2001).
20. A. Vardi, J.R. Anglin, Phys. Rev. Lett. **86**, 568 (2001); L. Pitaevskii, S. Stringari, `cond-mat/0104458`; J.R. Anglin, P. Drummond, A. Smerzi, `cond-mat/0011440`.
21. L.D. Landau, E.M. Lifshitz, *Quantum Mechanics*, 3rd edn. (Pergamon Press, Oxford, 1977); E. Merzbacher, *Quantum Mechanics*, 3rd edn. (John Wiley Sons Inc, 1998).
22. J.-Q. Liang, H.J.W. Müller-Kirsten, D.K. Park, F. Zimmerschied, Phys. Rev. Lett. **81**, 216 (1998).
23. J.-Q. Liang, Y.-B. Zhang, H.J.W. Müller-Kirsten, J.G. Zhou, F. Zimmerschied, F.-C. Pu, Phys. Rev. B **57**, 529 (1998).
24. J.-Q. Liang, H.J.W. Müller-Kirsten, Y.-B. Zhang, A.V. Shurgaia, S.P. Kou, D.K. Park, Phys. Rev. D **62**, 025017 (2000).
25. D.K. Park, H.J.W. Müller-Kirsten, J.-Q. Liang, Nucl. Phys. B **578**, 728 (2000).
26. A.L. Fetter, D.L. Feder, Phys. Rev. A **58**, 3185 (1998); E. Lundh, C.J. Pethick, H. Smith, *ibid.* **55**, 2126 (1997).
27. B.P. Anderson, M.A. Kasevich, Science **282**, 1686 (1998).
28. C. Orzel, A.K. Tuchman, M.L. Fenselau, M. Yasuda, M.A. Kasevich, Science **291**, 2386 (2001).
29. J. Williams, Phys. Rev. A **64**, 013610 (2001).
30. L. Salasnich, A. Parola, L. Reatto, Phys. Rev. A **60**, 4171 (1999); J. Williams, R. Wasler, I. Cooper, E. Cornell, M. Holland, *ibid.* **59**, R31 (1999).
31. E. Gildener, A. Patrascioiu, Phys. Rev. D **16**, 423 (1977).
32. J.-Q. Liang, H.J.W. Müller-Kirsten, Phys. Rev. D **46**, 4685 (1992).
33. N.S. Manton, T.S. Samols, Phys. Lett. B **207**, 179 (1988).
34. P. Achuthan, H.J.W. Müller-Kirsten, A. Wiedemann, Fortschr. Phys. **38**, 77 (1990).
35. F.S. Cataliotti, S. Burger, C. Fort, P. Maddaloni, F. Minardi, A. Trombettoni, A. Smerzi, M. Inguscio, Science **293**, 884 (2001).
36. A. Trombettoni, A. Smerzi, Phys. Rev. Lett. **86**, 2353 (2001).